

Contents lists available at ScienceDirect

Scripta Materialia

journal homepage: www.elsevier.com/locate/scriptamat



Abnormal twin-twin interaction in an Mg-3Al-1Zn magnesium alloy processed by laser shock peening



Bo Mao ^a, Yiliang Liao ^{a,*}, Bin Li ^{b,*}

- ^a Department of Mechanical Engineering, University of Nevada, Reno, Reno, NV 89557, USA
- ^b Department of Chemical and Materials Engineering, University of Nevada, Reno, Reno, NV 89557, USA

ARTICLE INFO

Article history: Received 25 January 2019 Received in revised form 16 February 2019 Accepted 18 February 2019 Available online xxxx

Keywords: Twin-twin interactions Ultra-high strain rate Magnesium alloys

ABSTRACT

Twin-twin interaction in an Mg-3Al-Zn1 magnesium alloy subjected to ultra-high strain rate deformation (\sim 10⁶/s) was investigated. The material was processed by laser shock peening and the microstructure at various depths was characterized by electron backscattered diffraction. The results show that different $\{10\overline{1}2\}$ twin variants were activated in individual parent grains, and the interfaces between these twin variants present very abnormal morphologies. One variant can be totally surrounded by the other, forming isolated or disconnected islands which have the same crystallographic orientation. A mechanism was proposed to account for the abnormal twin-twin interaction.

© 2019 Acta Materialia Inc. Published by Elsevier Ltd. All rights reserved.

 $\{10\overline{12}\}\langle10\overline{11}\rangle$ twinning plays an important role during plastic deformation of Mg alloys and has been extensively studied in the past decades [1–3]. It can be easily activated when a Mg crystal is subjected to tensile stress along the c-axis and results in a lattice orientation of 86.3° around $\langle1\overline{2}10\rangle$ zone axis [4]. Under some loading circumstances, multiple twin variants can be activated simultaneously and interact with each other, leading to twin-twin interaction. Recent studies show that twin-twin interaction has an important impact on twin propagation, de-twining, and twinning-induced strain hardening effect of Mg alloys [5–8].

Due to its scientific significance, experimental and numerical studies have been carried out to investigate twin-twin interactions of Mg alloys. For instance, Yu et al. [9] proposed that when two twin crystals with large misorientation angles interact with each other, their slip transmission is difficult. Chen et al. [10] reported that when a twin variant propagates and impinges on another, its growth will be retarded at the location of impingement, but the retardation depends on the angle between the sides of the intersecting twins. Gong et al. [11] studied the non-co-zone twin-twin interactions via atomistic simulations and showed that the growth of both twins is impeded upon interaction.

Despite these works, little efforts have been made to investigate twin-twin interaction in Mg alloys under ultra-high strain rate deformation (\sim 10⁶/s). The twinning behavior might be affected by the strain rate [12,13] and additional twinning modes could be activated and interact with each other with a higher strain rate [14]. Thus, it is of importance

* Corresponding authors. E-mail addresses: yliao@unr.edu (Y. Liao), binl@unr.edu (B. Li). to explore twin-twin interaction in Mg alloys under extreme deformation conditions.

Laser shock peening (LSP) is a surface treatment technique that has been widely used to study high strain-rate response of metallic materials [15–17]. During LSP, pulsed laser with an ultra-short duration (on an order of nanosecond) is delivered to an ablative coating, forming a high-temperature plasma and generating a high shockwave pressure (on the order of GPa) on the sample being processed. As the shockwave propagates into the target materials, the near surface layer (typically 0–2000 μm) undergoes an ultra-high strain rate plastic deformation [16,18]. In this work, twin-twin interaction in an AZ31B Mg alloy under ultra-high strain rate compression introduced by LSP was studied. The morphology of twin variants was characterized by electron backscattering diffraction (EBSD) characterization. Very interesting results were obtained.

Samples for LSP experiments were cut from a rolled AZ31B Mg block (3.0 wt% Al, 1.0 wt% Zn, Mg balance) purchased from Metalmart.com. Prior to LSP, the surface containing the normal direction (ND) and the transverse direction (TD) of the sample was mechanically grinded with a series of sand papers (down to 1200 grit number) followed by a final polishing using 3 µm diamond suspension. A detailed description of the LSP process can be found in the Supplementary information. The examined RD-TD cross section was cut along the diameter direction of the laser beam spot by a low-speed diamond saw and then prepared for EBSD characterization.

The initial microstructure and texture of the RD-TD cross-section of the as-received Mg alloy sample before LSP is shown in Fig. 1a. It can be seen that, before LSP, the material has a twin-free, equiaxed grain structure with a strong basal texture. After LSP, EBSD analysis was performed at the depths of 500, 700, 900 and 1100 μm from the processed surface

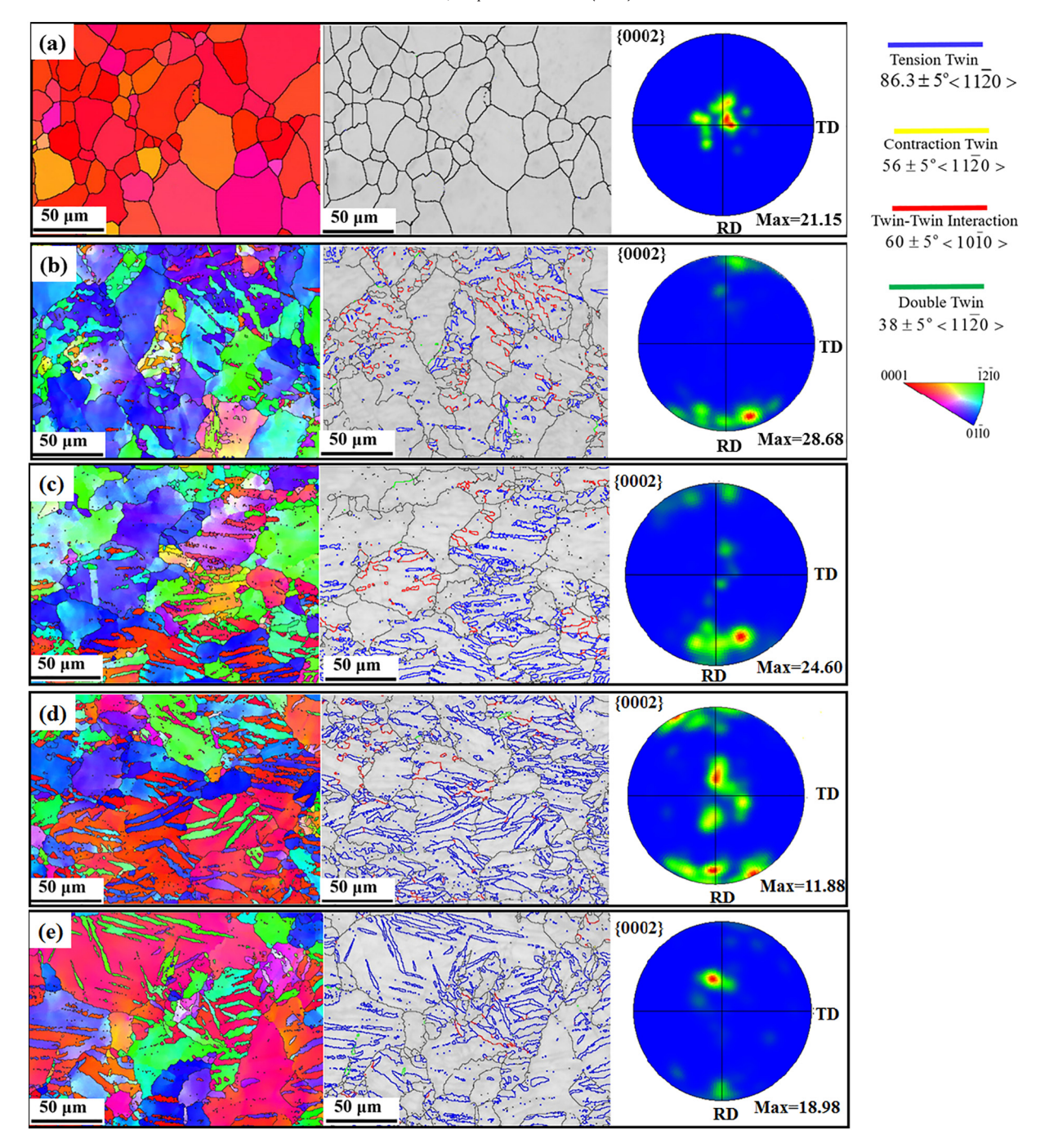


Fig. 1. (a) Microstructure and texture of the as-received AZ31B Mg alloy. (b–e) Evolution of microstructure and texture at various depths from the laser processed surface: (b) 500 μ m; (c) 700 μ m; (d) 900 μ m; (e) 1100 μ m. The twin volume fraction decreases with increasing depth. The density of $60 \pm 5^{\circ} (10\overline{10})$ boundaries (in red) also decreases with increasing depth. (For interpretation of the references to color in this figure legend, the reader is referred to the web version of this article.)

and the results are shown in Fig. 1b–e. From the inverse pole figure (IPF) maps and the (0002) pole figures, it can be seen that $\{10\overline{1}2\}$ extension twinning was activated. Close to the surface, the parent grains were nearly all twinned (Fig. 1b), because the loading condition strongly favors $\{10\overline{1}2\}\langle10\overline{11}\rangle$ twinning [3]. Due to the attenuation of the laser intensity [19], the twin volume fraction decreases with depth. To characterize the nature of interfaces, we highlight different types of grain boundaries with different colors in the image quality maps: the blue lines represent twin boundaries (TBs) of $86.3 \pm 5^{\circ}\langle11\overline{2}0\rangle$, characteristic of $\{10\overline{1}2\}$ extension twins; the yellow lines represent TBs of $56 \pm 5^{\circ}\langle11\overline{2}0\rangle$ from $\{10\overline{1}1\}$ contraction twins which have a

very low density; a few green lines of $38 \pm 5^{\circ} \langle 11\overline{2}0 \rangle$ can also be seen, which represent $\{10\overline{1}1\} + \langle 10\overline{1}2 \rangle$ double twins. Notably, a quite high density of red boundaries can be identified in the LSP affected areas. These are $60 \pm 5^{\circ} \langle 10\overline{1}0 \rangle$ boundaries formed when different $\{10\overline{1}2\}$ twin variants impinge [9,20]. The density of $60 \pm 5^{\circ} \langle 10\overline{1}0 \rangle$ boundaries decreases with increasing depth, indicating that multiple $\{10\overline{1}2\}$ twin variants were activated and strongly interacted with each other during LSP processing. More detailed analysis of the twin variants their orientations are provided below.

EBSD scans with a higher resolution were then performed in selected areas which contain multiple twin variants such that details of twin-twin interaction can be better revealed. The red patches, marked as M, are the leftover of parent grains that are not totally twinned. These parent grains contain two twin variants: T_1 and T_2 (Fig. 2a). The image quality map (Fig. 2b) and crystallographic orientation analysis (Fig. 2c–d) indicate that the interfaces between T_1 and T_2 are $60\pm5^\circ\langle 1\ 0\overline{1}0\rangle$ type, which result from twin-twin interaction. Secondary twins can also be observed. For example, T_3 is another primary twin variant and this variant was transformed to secondary twins T_4 and T_5 . Note that the boundary between T_4 and T_5 also satisfies $60\pm5^\circ\langle 10\overline{1}0\rangle$. The unit cells and crystallographic relationship among M, T_3 , T_4 , and T_5 is shown in Fig. 2e.

A salient feature of the boundaries resulting from twin-twin interaction induced by ultra-high strain rate deformation is the closed, circular interfaces, as shown in Fig. 3. Highly irregular interfaces between $\{10\overline{1}2\}$ twin variants were only recently reported by Chen et al. [20] in an AZ31 Mg alloys with very coarse grains (~120 μm). Fig. 3a–b shows several isolated twin variants of T_2 that are surrounded by variant T_1 . The misorientation angle between variant T_1 and T_2 satisfies $60\pm5^\circ(10\overline{1}0$ \rangle , as shown in the image quality map in Fig. 3b. The parent grain has almost been totally twinned into variant T_1 . It is likely that during twin growth, variant T_1 outgrew the twin lamella of T_2 and then totally enclosed T_2 inside. As the interaction continued, part of the T_2 may have been transformed to T_1 , leading to the disconnected, abnormal

morphology. A similar scenario is shown in Fig. 3c and d in which some disconnected islands can be observed. These disconnected islands belong to the same twin variant T₄.

The abnormal morphology of the interface between different twin variants simply cannot be explained by any twinning dislocation theories because, by definition, a twinning dislocation can only glide on the twinning plane and produce a simple shear. When two or more variants approach each other, the stress field of the twinning dislocations of one twin variant will repel the twinning dislocations of the other twin variants, if we assume the interfaces between a twin variant and the matrix are composed of a multitude of twinning dislocation loops on consecutive twinning planes and lateral growth of the twin is controlled by the expansion of the loops [2]. Thus, it is unlikely that, as one variant impinges on a different variant, the growth front of the incident variant branches out and changes the habit plane. This is exactly the case in twinning in FCC and BCC metals, as schematically demonstrated in Fig. 4a. The expansion of twins has to halt when two variants approach close to each other because the twinning dislocations cannot penetrate the twin boundaries. As a result, the parent grains cannot be twinned by 100%. To account for the fact that parent grains can be totally twinned by $\{10\overline{12}\}$ twinning in HCP metals, Song and Gray [21] first questioned the twinning dislocation theories in which $\{10\overline{1}2\}$ is mediated by twinning dislocations just like other twinning modes. They proposed that the growth of $\{10\overline{1}2\}$ twins was controlled by coordinated movements

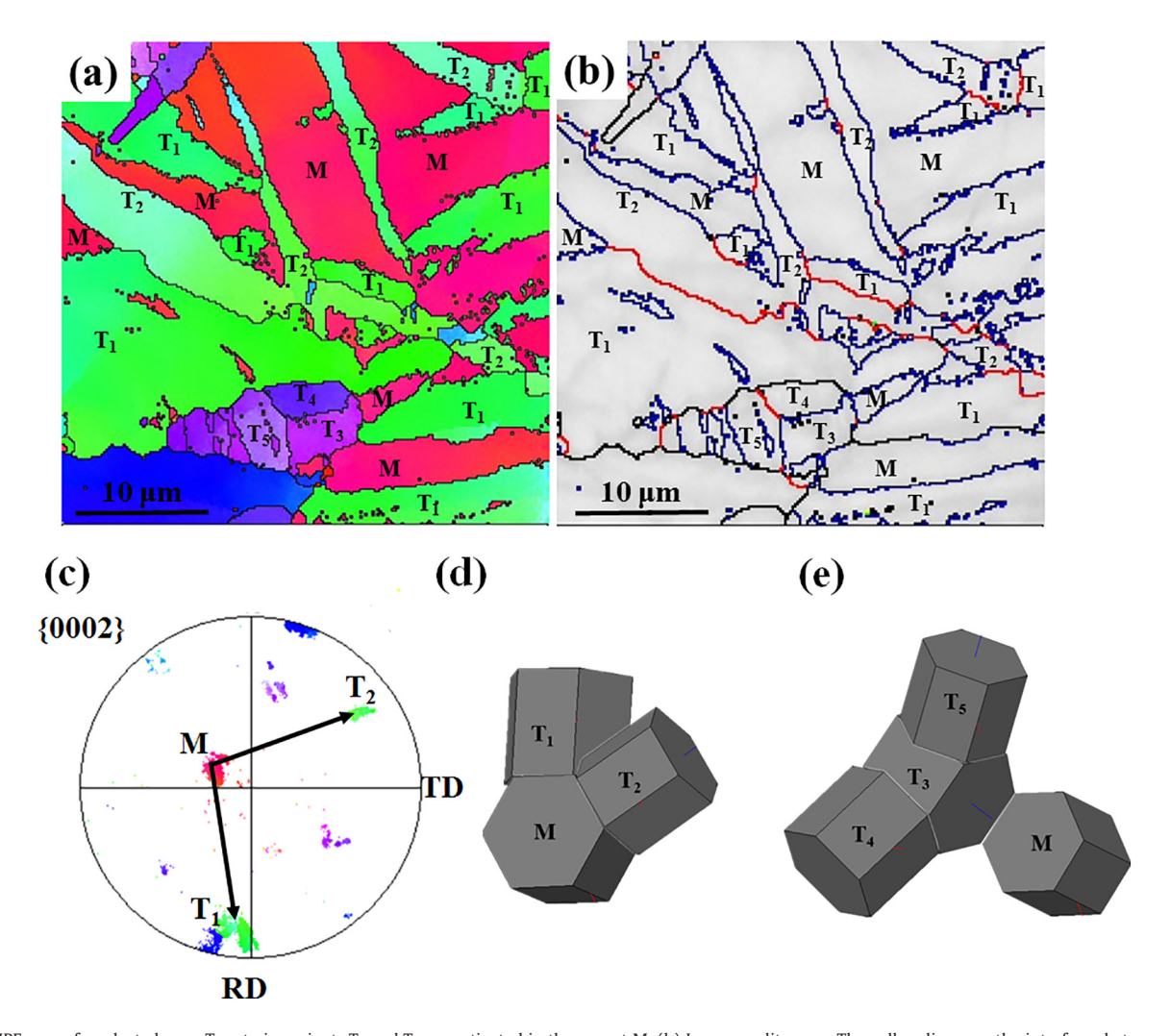


Fig. 2. (a) IPF map of a selected area. Two twin variants T_1 and T_2 are activated in the parent M. (b) Image quality map. The yellow lines are the interfaces between T_1 and T_2 . (c) Corresponding (0002) pole figure. (d) Unit cells of the parent M, and the two twin variants T_1 and T_2 . (e) Unit cells of parent M, primary twin variant T_3 , and two secondary twin variants T_4 and T_5 . (For interpretation of the references to color in this figure legend, the reader is referred to the web version of this article.)

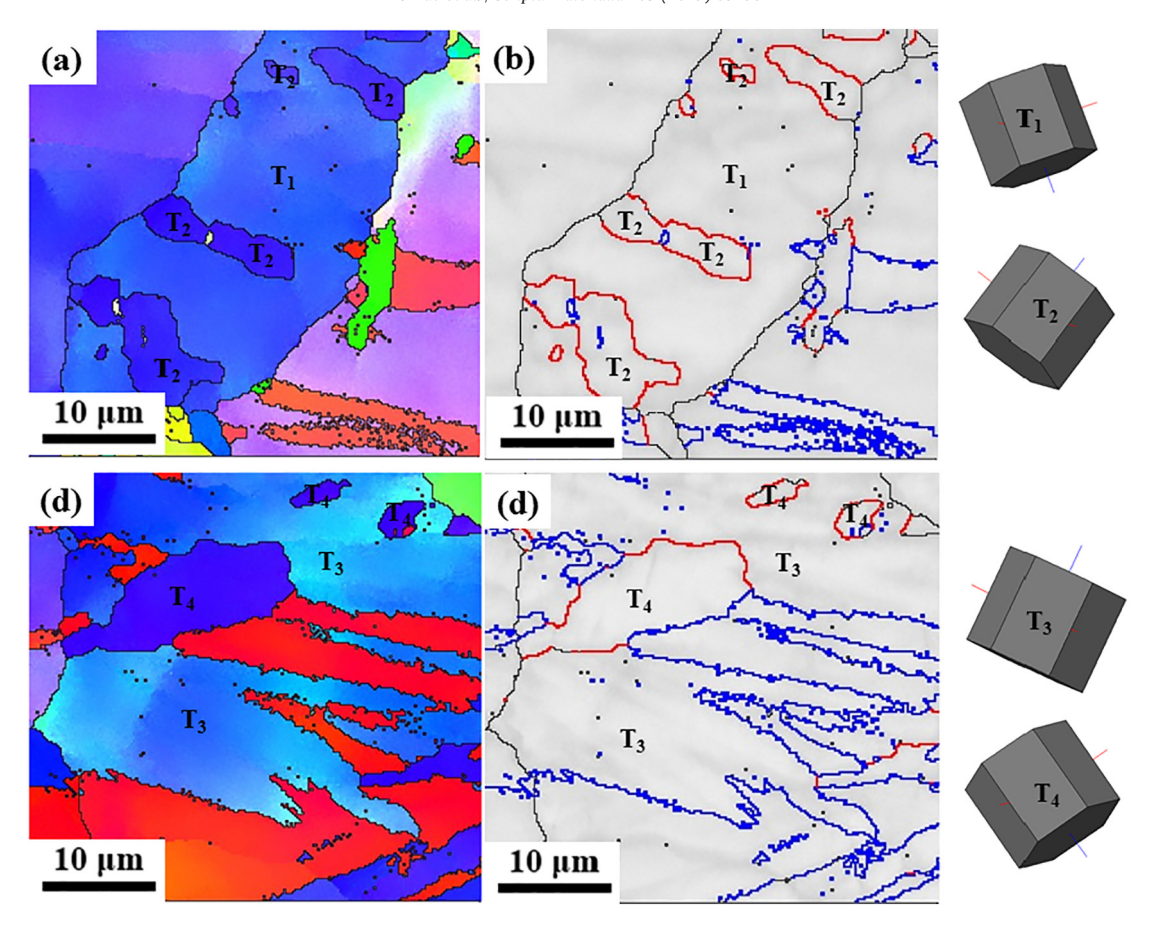


Fig. 3. (a) Twin variant T_2 is surronded by twin variant T_1 , leading to the isolated T_2 islands in a parent grain. (b) Image quality map of (a). (c) Twin variants T_4 is surronded by twin variant T_3 , leading to isolated T_4 islands in another grain. (d) Image quality map of (c).

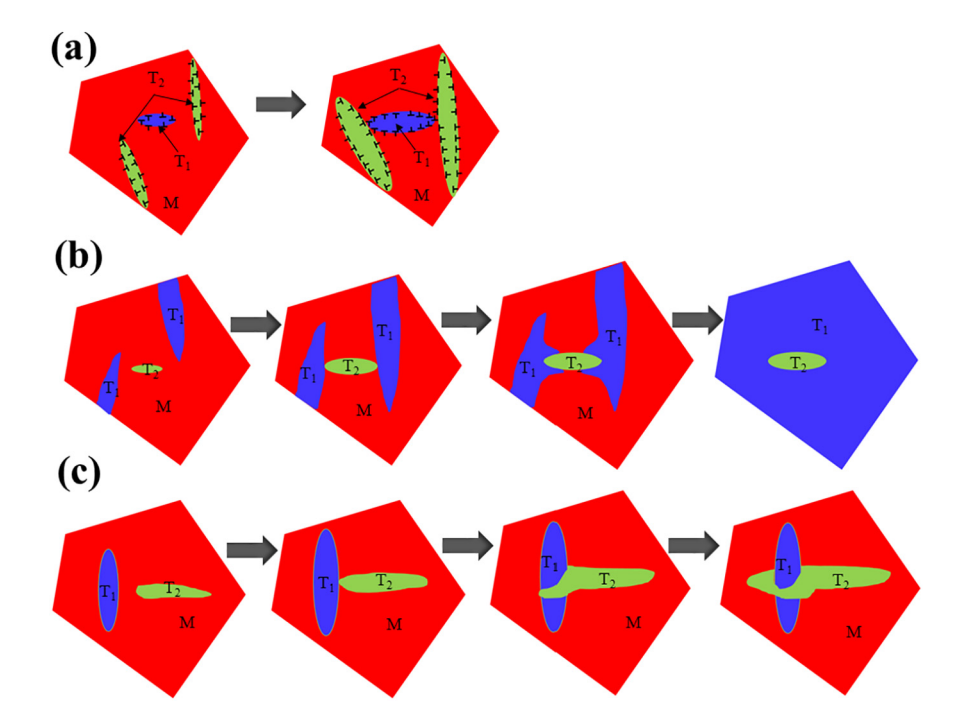


Fig. 4. (a) Twin-twin interaction when growth of the twin variants is controlled by twinning dislocations on the twin boundaries. The growth of the twin variants will be impeded as the variants approach close to each other because the twinning dislocations are unable to penetrate the twin boundaries. (b) Non-dislocation mediated twin growth. A twin variant can branch out by changing the habit plane and surround the other variant. Eventually, the parent grain can be totally twinned. (c) Non-dislocation mediated twin growth. A twin variant can spread laterally and grow around the other variant, forming an "apparent crossing" structure.

of a large number of atoms rather than by twinning dislocations gliding on the twinning plane.

Recently, Li and Ma [22] proposed that $\{10\overline{1}2\}$ twinning is mediated purely by atomic shuffling, not by twinning dislocations. The atomic shuffles transform the parent basal plane to the twin prismatic plane and vice versa, without involving any twinning dislocations. More recently, Li and Zhang [23] proved that the $\{10\overline{1}2\}$ twinning plane is not an invariant plane. Consequently, no twinning shear can occur on the twinning plane. As such, $\{10\overline{1}2\}$ twin boundaries can be extremely incoherent, as confirmed by numerous experimental studies [24-29]. The abnormal interfacial structure between different $\{10\overline{1}2\}$ twin variants can be well explained by these non-twinning-dislocation models. As shown in Fig. 4b, two or more twin variants are activated inside a parent grain. As observed in extensive transmission electron microscopy (TEM) experiments, the twin boundaries can be extremely incoherent, although microscopically the twin variants still assume a lamellar shape [27,30–32]. As the twin variants approach each other, one variant may impinge on the other. However, the twin growth is not halted by the impingement. Instead, one variant can branch out and change the habit plane because no twinning dislocations are gliding on the twin boundary which should coincide with the twinning plane according to classical twinning theory. As a result of such non-classical twin growth, a parent grain can be twinned 100% and a twin variant can be totally surrounded by another variant.

Based on atomistic simulations, Serra et al. [33,34] proposed that $\{10\overline{1}2\}$ twinning is mediated by "disconnections" rather than zonal twinning dislocations. However, as analyzed in recent works [31,35] the lattice correspondence in the reports of "disconnections" is exactly the same as the Li-Ma shuffling model [36]. In fact, the "basal to prismatic and prismatic to basal" lattice transformation can be readily identified in most of the atomistic simulations in the literature. Such a transformation must distort the structure of the twinning plane and thus no twinning shear should occur on the twinning plane [23].

The abnormal interaction between different twin variants provides new insight on the non-classical twinning behavior that has been observed extensively in experimental studies. For example, Li et al. [37] observed in TEM that a twin variant was able to penetrate a grain boundary and extend into the neighboring grain. It is well known that a twinning dislocation cannot penetrate a grain boundary. The wellobserved "apparent crossing" during twin-twin interaction [6-9,38] in Mg alloys and other HCP metals can now be well explained. Shi et al. [6] showed that when one twin impinges on another twin lamella, it looks like that a new twin with the same crystallographic orientation emerges on the other side of the impinged lamella. Mokdad et al. [7] also observed that impinging twins were linked on each side of twin lamella. Similar observation is also found in Fig. 2a-b, in which two twin variants T₁ are linked on each side of T₂. A schematic explanation of these phenomena is shown in Fig. 4c, when two $\{10\overline{1}2\}$ twin variants impinge, one variant can spread laterally and grow around the other variant. When a cross-sectional view is made, it looks like that one variant crosses the other.

In summary, we investigated the twin-twin interactions in an AZ31B magnesium alloy subjected to ultra-high strain rate deformation by laser shock peening. EBSD characterization of the interfaces between different $\{10\overline{1}2\}$ twin variants shows that these interfaces present abnormal morphologies that cannot be accounted for by twinning dislocation theories. Patches of one variant can be completely surrounded by

another variant. Such an abnormal behavior of twin-twin interaction can only be explained by non-twinning-dislocation theories that fundamentally differ from the classical twinning theory.

Acknowledgements

Y. Liao appreciates the financial support by startup funding from the Department of Mechanical Engineering at the University of Nevada, Reno. Bin Li thanks support from U.S. National Science Foundation (CMMI-1635088 and CMMI-1726897).

Appendix A. Supplementary data

Supplementary data to this article can be found online at https://doi.org/10.1016/j.scriptamat.2019.02.028.

References

- [1] M. Niewczas, Acta Mater. 58 (17) (2010) 5848-5857.
- [2] J.W. Christian, S. Mahajan, Prog. Mater. Sci. 39 (1) (1995) 1-157.
- [3] A. Khosravani, D. Fullwood, B. Adams, T. Rampton, M. Miles, R. Mishra, Acta Mater. 100 (2015) 202–214.
- [4] M. Barnett, Mater. Sci. Eng. A 464 (1-2) (2007) 1-7.
- [5] H. El Kadiri, J. Kapil, A. Oppedal, L. Hector Jr., S.R. Agnew, M. Cherkaoui, S. Vogel, Acta Mater. 61 (10) (2013) 3549–3563.
- [6] D. Shi, T. Liu, D. Hou, H. Chen, F. Pan, H. Chen, J. Alloys Compd. 685 (2016) 428-435.
- 7] F. Mokdad, D. Chen, D. Li, Mater. Des. 119 (2017) 376–396.
- [8] B. Morrow, E. Cerreta, R. McCabe, C. Tomé, Mater. Sci. Eng. A 613 (2014) 365–371.
- [9] Q. Yu, J. Wang, Y. Jiang, R.J. McCabe, N. Li, C.N. Tomé, Acta Mater. 77 (2014) 28–42.
- [10] H. Chen, T. Liu, S. Xiang, Y. Liang, J. Alloys Compd. 690 (2017) 376–380.
- [11] M. Gong, S. Xu, Y. Jiang, Y. Liu, J. Wang, Acta Mater. 159 (2018) 65-76.
- [12] N. Dudamell, P. Hidalgo-Manrique, A. Chakkedath, Z. Chen, C. Boehlert, F. Gálvez, S. Yi, J. Bohlen, D. Letzig, M. Pérez-Prado, Mater. Sci. Eng. A 583 (2013) 220–231.
- [13] K. Hazeli, V. Kannan, O. Kingstedt, G. Ravichandran, K. Ramesh, arXiv preprint, arXiv: 1801.10252 2018.
- [14] M. Wang, L. Lu, C. Li, X. Xiao, X. Zhou, J. Zhu, S. Luo, Mater. Sci. Eng. A 661 (2016) 126–131.
- [15] R. Ecault, L. Berthe, F. Touchard, M. Boustie, E. Lescoute, A. Sollier, H. Voillaume, J. Phys. D. Appl. Phys. 48 (9) (2015) 095501.
- [16] P. Peyre, R. Fabbro, Opt. Quant. Electron. 27 (12) (1995) 1213-1229.
- [17] B. Mao, A. Siddaiah, P.L. Menezes, Y. Liao, J. Mater. Process. Technol. 257 (2018) 227–233.
- [18] B. Mao, Y. Liao, B. Li, Appl. Surf. Sci. 457 (2018) 342–351.
- [19] X. Zeng, X. Mao, S.S. Mao, S.-B. Wen, R. Greif, R.E. Russo, Appl. Phys. Lett. 88 (6) (2006) 061502.
- [20] P. Chen, F. Wang, J. Ombogo, B. Li, Mater. Sci. Eng. A, 739 (2018) 173–185.
- [21] S. Song, G. Gray III, Acta Metall. Mater. 43 (6) (1995) 2325–2337.
- [22] B. Li, M. Sui, B. Li, E. Ma, S. Mao, Phys. Rev. Lett. 102 (20) (2009) 205504.
- [23] B. Li, X. Zhang, Scr. Mater. 125 (2016) 73-79.
- [24] P. Partridge, E. Roberts, Acta Metall. 12 (11) (1964) 1205–1210.
- [25] Q. Ma, B. Li, E. Marin, S. Horstemeyer, Scr. Mater. 65 (9) (2011) 823–826.
- [26] P. Molnár, A. Jäger, P. Lejček, Scr. Mater. 67 (5) (2012) 467-470.
- 27] X. Zhang, B. Li, X. Wu, Y. Zhu, Q. Ma, Q. Liu, P. Wang, M. Horstemeyer, Scr. Mater. 67 (10) (2012) 862–865.
- [28] J. Wang, S. Yadav, J. Hirth, C. Tomé, I. Beyerlein, Mater. Res. Lett. 1 (3) (2013) 126–132.
- [29] Y. Cui, Y. Li, S. Sun, H. Bian, H. Huang, Z. Wang, Y. Koizumi, A. Chiba, Scr. Mater. 101 (2015) 8–11.
- [30] N.L.Y. Liu, S. Shao, M. Gong, J. Wang, R.J. McCabe, Y. Jiang, Nat. Commun. 7 (2016).
- [31] X. Zhang, B. Li, Q. Sun, Scr. Mater. 159 (2019) 133–136.
- [32] J. Jeong, M. Alfreider, R. Konetschnik, D. Kiener, S.H. Oh, Acta Mater. 158 (2018) 407–421.
- [33] A. Serra, D. Bacon, Philos. Mag. A 73 (2) (1996) 333-343.
- 34] A. Serra, D. Bacon, Philos. Mag. A 54 (6) (1986) 793-804.
- [35] P. Chen, F. Wang, B. Li, Acta Mater. 164 (2019) 440-453.
- [36] B. Li, E. Ma, Phys. Rev. Lett. 103 (3) (2009) 035503.
- [37] B. Li, E. Ma, K. Ramesh, Metall. Mater. Trans. A 39 (11) (2008) 2607–2614.
- [38] F. Mokdad, D. Chen, D. Li, J. Alloys Compd. 737 (2018) 549-560.